10 August 2001

ELSEVIER

Chemical Physics Letters 343 (2001) 535–542

CHEMICAL
PHYSICS
LETTERS

www.elsevier.com/locate/cplett

Ab initio computation of molecular singlet–triplet energy differences using auxiliary field Monte Carlo

Roi Baer *

Department of Physical Chemistry, Lise Meitner Minerva Center for Quantum Chemistry, The Hebrew University of Jerusalem, Jerusalem 91904, Israel

Received 8 February 2001; in final form 8 June 2001

Abstract

A method for computing the singlet–triplet energy difference (STED) of molecules with nearly degenerate states is described. It is based on the shifted contour auxiliary field Monte Carlo, implemented with plane waves and pseudopotentials. Two additional critical elements are: a variational multireference approach, for treating non-dynamical correlation and direct correlated sampling of energy differences. Applications to the H–He–H and CH_2 systems are given, estimating STED of -14.3 ± 0.1 and 9.8 ± 0.3 kcal/mol, respectively. The overall accuracy is limited by the type of pseudopotential used, with preference to those based on generalized gradients. © 2001 Elsevier Science B.V. All rights reserved.

1. Introduction

The characterization and description of magnetic–exchange interactions in molecules and solids is a highly active research area of modern experimental chemistry extending applications to a variety of fields in inorganic chemistry, materials science and bioorganic chemistry. Exchange-active molecules exhibit a manifold of nearly degenerate electronic states determining the magnetic properties of the material. A frequently used phenomenological model for studying the behavior of magnetic systems is the Heisenberg Hamiltonian [1] $H = -\sum_{ab} J_{ab}\mathbf{S}_a\cdot\ \mathbf{S}_b$, accentuating spin–spin interactions, where each spin $\mathbf{S}_a$ is located at a site a of the magnetic solid. Magnetic systems are generally classified as ferromagnetic or antiferromagentic according to their tendency to develop or destroy a collective magnetic moment. It is clear from the form of the Heisenberg interaction that predominantly positive phenomenological magnetic coupling constants J_{ab} lead to ferromagnetic behavior, while negative constants promote antiferromagnetism.

The phenomenological magnetic coupling constants can be determined directly from ab initio electronic structure theory, applied to a single dimer $H_{ab} = -J_{ab}\mathbf{S}_a \cdot \mathbf{S}_b$. The eigenstates are characterized by eigenvalues of $\mathbf{S}^2 = (\mathbf{S}_a + \mathbf{S}_b)^2$, $\mathbf{S}_a^2$ and $\mathbf{S}_b^2$ so that for a given pair of spins, S_a and S_b, the energy manifold consists of states with total spin $S = |S_a - S_b|, \dots S_a + S_b$ and the Heisenberg energy eigenvalues are:

$$E(S, S_a, S_b) = \frac{-J_{ab}}{2}[S(S+1) - S_a(S_a+1) - S_b(S_b+1)]. \qquad (1)$$

---

* Fax: +972-2-651-3742.
E-mail address: roi.baer@huji.ac.il (R. Baer).

PII: S0009-2614(01)00723-0

Thus, J_{ab} can be estimated from ab initio computation of the energy difference between adjacent spin states [2]

$$J_{ab} \approx -\frac{E(S, S_a, S_b) - E(S-1, S_a, S_b)}{S}. \tag{2}$$

The most common use of this equation is the case of $S = 1$, leading to a connection of the magnetic coupling with STED

$$J = E(\text{singlet}) - E(\text{triplet}). \tag{3}$$

In this Letter, we discuss a new method for computing the high accuracy singlet–triplet energetic difference in molecules. The methods presented are based on the shifted contour auxiliary field quantum Monte Carlo method (SC-AFMC) [3,4]. In previous publications, we showed that SC-AFMC can be implemented using correlated fields and this technique allows the computation of forces, deformation barriers and spectroscopic constants of molecules [5,6]. Here, we demonstrate that correlated sampling SC-AFMC is applicable to the computation of STED.

We study the methods for computing STED with application to two molecular systems. First, we treat the collinear H–He–H complex biradical (Section 3.1). This is the simplest model for super-exchange a known benchmark for testing broken symmetry [7] and associated approximations to the magnetic coupling constants (for a comprehensive review on broken symmetry the reader is referred to Ruiz et al. [8]). We find that the non-dynamical correlation dominates the problem and single-reference SC-AFMC is extremely inefficient and impractical. Thus, a multireference formalism, similar to that of Bernu et al. [9] and Rom et al. [10] is developed (Section 2.2) emphasizing the variational properties of the method. The multireference method, together with the correlated sampling, is applied to the system and the Monte Carlo process used in two differently related samplings is applied to the system and the Monte Carlo process is used in two different ways to compute the same STED.

Finally, we apply the method to the CH_2 radical (Section 3.2). Here, non-dynamical correlation is less of a problem, however, the fact that the triplet state is lower in energy than the singlet state, causes a strong mixing in the open-shell $S_z = 0$ reference which precludes the use of open-shell references for the singlet.

2. Theory

2.1. Shifted contour auxiliary field Monte Carlo

Consider a system of interacting electrons, with the following Hamiltonian, in second quantization form:

$$\hat{H} = K^{\mathrm{T}}\rho + \frac{1}{2}\rho^{\mathrm{T}}V\rho, \tag{4}$$

where $\hat{\rho}(\mathbf{r}) = \sum_{s=\uparrow\downarrow}\psi_s^\dagger(\mathbf{r})\psi_s(\mathbf{r})$ is the electron density operator, $V(\mathbf{r},\mathbf{r}') = e^2|\mathbf{r}-\mathbf{r}'|^{-1}$ is the positive Coulomb repulsion and K a one-body term, including the kinetic energy, the external potential, and the other one-body interaction terms. We use here the notation

$$\rho^{\mathrm{T}}V\rho \equiv \int \rho(\mathbf{r})\frac{\mathrm{e}^2}{|\mathbf{r}-\mathbf{r}'|}\rho(\mathbf{r}')\,\mathrm{d}^3r\,\mathrm{d}^3r'. \tag{5}$$

For a N_{e} electron system, the auxiliary field Monte Carlo specializes in computing the following types of matrix elements:

$$\mathbf{S}_{m'm} = \langle \Phi_{m'}|\mathrm{e}^{-\beta\hat{H}}|\Phi_m\rangle \tag{6}$$

and

$$\mathbf{H}_{m'm} = \langle \Phi_{m'}|\hat{H}\mathrm{e}^{-\beta\hat{H}}|\Phi_m\rangle, \tag{7}$$

where Φ_m is a N_{e}-electron determinantal wavefunction. It is enough to focus on Eq. (6) because the other type of matrix elements can be obtained, for example, by differentiation

$$\mathbf{H}(\beta) = -\mathbf{S}'(\beta). \tag{8}$$

Computing these matrix elements is extremely demanding because of the two-body part of the Hamiltonian $\hat{H}$. This feat can be made tractable using the shifted contour auxiliary field approach, details and references of which are supplied in [4,11]. The matrix elements are computed using the following Monte Carlo procedure summarized by the following equation:

$$\mathbf{S}_{m'm}(\beta) = \mathrm{e}^{1/2\alpha_m^{\mathrm{T}} V \alpha_m \beta} \left\langle \langle \Phi_{m'} | \prod_{n=1}^{N} \mathrm{e}^{-\mathrm{i}\alpha_m^{\mathrm{T}} V \sigma_n \Delta\beta} \times \mathrm{e}^{-\Delta\beta (K + \mathrm{i} V \sigma_n(\mathbf{r}))^{\mathrm{T}} \hat{\rho}} | \Phi_m \rangle \right\rangle_{W\{\sigma\}}. \tag{9}$$

Here the β-time interval is sampled by N equally spaced time points $\beta_n = n\Delta\beta \ (n = 0, 1, \ldots, N)$ where $\Delta\beta = \beta/N$. At each time point β_n, a three-dimensional real density $\sigma_n(\mathbf{r})$ is randomly generated by a standard process assuring a distribution adhering to the positive definite Gaussian weight

$$W\{\sigma_n(\mathbf{r})\} = \mathrm{e}^{-1/2 \sum_{n=1}^{N} \sigma_n^{\mathrm{T}} V \sigma_n \Delta\beta}. \tag{10}$$

The real function $\alpha_m(\mathbf{r})$ is the contour shift designed for reducing the statistical noise of the Monte Carlo process [3,4]. It was shown that the ideal shift is time-dependent and depends on both the left and right states

$$\alpha(\mathbf{r}, \tau) = \langle \Phi_{m'} | \mathrm{e}^{-\hat{H}(\beta - \tau)} \rho(\mathbf{r}) \mathrm{e}^{-\hat{H}\tau} | \Phi_m \rangle. \tag{11}$$

However, accurate determination of this quantity is as difficult as computing **S**. Thus, an approximate shift is adopted. It should be noted that, similar to the concept of importance sampling, the result is in principle independent of the shift α. Yet, the statistical variance can be substantially reduced if a suitable approximation to Eq. (11) is made. In this Letter we use the following shift:

$$\alpha_m(\mathbf{r}) = \langle \Phi_m | \rho(\mathbf{r}) | \Phi_m \rangle \tag{12}$$

The fact that α depends only on the right-hand side function greatly facilitates the computation. The importance in using a contour shift cannot be overestimated and computations which have not utilized it have had very limited success with this method [12,13].

Once the contour shift $\alpha_m(\mathbf{r})$ has been determined and the random densities $\sigma_n(\mathbf{r})$ have been generated, the evolution is executed on each of the one-electron orbitals in the determinant Φ_m. The fact that the effective Hamiltonian in Eq. (9) is a one-body Hamiltonian means that each orbital can be evolved independently of the others.

2.2. Variational multireference AFMC

For some systems, non-dynamical correlation is important and a multireference version of AFMC is needed. We follow the approach, inspired by the work of Bernu et al. [9] and suggested also by Rom et al. [10]. Our derivation emphasizes the variational properties of the method.

Consider a set of M determinantal wavefunctions $\Phi_m(\xi_1, \ldots, \xi_{N_e})$, $m = 1, \ldots, M$, the choice of which is application-dependent, as discussed in the next section. Here ξ_n are the coordinates and spin of the nth electron.

Projecting with the Boltzmann operator, damping the high-energy components, a new set of M functions is obtained

$$\Phi_m(\beta) = \mathrm{e}^{-\beta\hat{H}} \Phi_m. \tag{13}$$

A linear combination of the resulting wavefunctions can efficiently approximate the true ground-state wavefunction:

$$\Psi_{\mathrm{gs}} \approx \Psi = \sum_{m=1}^{M} C_m \Phi_m(\beta). \tag{14}$$

The coefficients C_m are determined by the variational principle, according to which

$$E_{\mathrm{gs}} \leqslant \langle \Psi | \hat{H} | \Psi \rangle \tag{15}$$

when $\langle \Psi | \Psi \rangle = 1$. Thus, the best coefficients are determined by minimizing the energy expectation value, subject to wavefunction normality. This amounts to minimizing the following functional:

$$J(\mathbf{C}) = \mathbf{C}^{\dagger}\mathbf{H}\mathbf{C} - \varepsilon\{\mathbf{C}^{\dagger}\mathbf{S}\mathbf{C} - 1\}, \tag{16}$$

where a matrix–vector notation is employed, for example

$$\mathbf{C}^{\dagger}\mathbf{S}\mathbf{C} = \sum_{m,m'=1}^{M} C_{m'}^{*} S_{m'm} C_m, \tag{17}$$

the Lagrange parameter ε multiplies the normalization constraint and the matrices appearing in Eq. (16) are defined in Eqs. (6) and (7), the estimation of which was discussed in the previous section. The constrained minimization leads to the following generalized eigenvalue equation:

$$\mathbf{H}\mathbf{C} = \mathbf{S}\mathbf{C}E, \tag{18}$$

where **E** is the diagonal matrix of Lagrange multipliers. The smallest Lagrange multiplier is the variational estimate for the ground state energy. Indeed, the following inequality exists in the limit of large β:

$$E_{\mathrm{gs}} \leqslant E(\beta) < E_{\mathrm{gs}} + E_{M+1} \mathrm{e}^{-\beta\left(E_{M+1}-E_{\mathrm{gs}}\right)}. \tag{19}$$

Estimates for low-lying excitation energies are given by the other diagonal elements of the matrix **E**.

3. Applications

We now present two applications of Auxiliary Field Monte Carlo to the computation of STED in molecular systems. The computations were all performed using a plane wave basis for the one-electron wavefunctions, where the molecule is placed in a cubic cell of length L, and a three-dimensional grid of spacing Δx. We use the technique of Martyna et al. [14] for efficiently mitigating finite cell size effects. All computations employ B-LYP [15,16]-based Troullier–Martins type [17] pseudopotentials, generated for hydrogen, carbon and helium by the FHIPP98 computer program of Fuchs and Scheffler [18]. All pseudopotentials are non-local with $l_{\max} = 2$ and the Kleinman–Bylander form [19] is used for their efficient application in the code.

3.1. H–He–H: Magnetic exchange benchmark system

The linear, symmetric system $\mathrm{H} \cdots \mathrm{He} \cdots \mathrm{H}$, is *not a* stable molecule, so there is no experimental determination of the STED. Yet, this is a four-electron system and it is amenable to reasonably accurate full CI treatments [20–22]. It is known then that when the hydrogen–helium distance $R_{\mathrm{H\text{–}He}}$ is large, a near-degenerate singlet–triplet manifold is seen and the result is an ideal benchmark system for testing various approximations of STED computation.

We study this system for the hydrogen–helium distance of $R_{\mathrm{H\text{–}He}} = 1.25$ Å. In the first encounter, we used two unrestricted Hartree–Fock (UHF) determinantal wavefunctions: one with $S_z = 0$, and the other with $S_z = 1$. In a naïve AFMC application, we applied correlated sampling for the two electronic states. This can be done because both determinants have the four orbitals, and the same auxiliary fields can be used for both. The results are shown in Fig. 1. The statistical error is well under control, due to the correlated sampling, however the STED converges very slowly. We might think from the figure that the converged value is about −8 kcal/mol however the correct value based on full CI computations [20,21,23] is about −14 kcal/mol. The reason for the large discrepancy is the improper treatment of the near degeneracy. The singlet UHF reference is strongly spin-contaminated by the lowest triplet state. All ‘broken symmetry’ type approximations are based on just this phenomenon [8]. Since the STED is around 0.02 Ht, the time scale for the Monte Carlo process to resolve this difference is $\beta \gg 50$ a.u. The way to correctly and efficiently compute the STED is to use the multireference theory of Section 2. This leads to two independent ways of computing the STED.

We begin by considering the UHF $S_z = 0$ reference $\Phi_1 = |\phi_1\bar{\phi}_2\phi_3\bar{\phi}_4|$. The two optimized orbitals ϕ_3 and $\bar{\phi}_4$ are each localized on a different

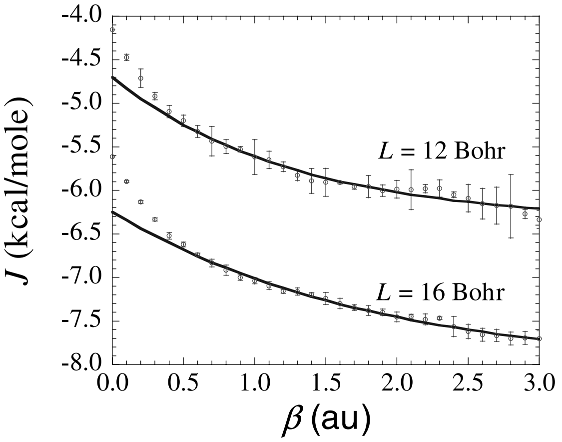

Fig. 1. A slowly convergent computation of the STED for H–He–H, with H–He distance equal to 1.25 Å. The STED of this system is known to be around 14 kcal/mol. At this rate, convergence will be reached after $\beta = 50$ a.u. Solid lines are exponentials best fitted to the data for $\beta > 0.5$ a.u. The effect of increasing the cubic cell length L is also shown.

hydrogen atom but otherwise, they are similar. Thus, the spin-exchanged determinant $\Phi_2 = |\phi_1\bar{\phi}_2\bar{\phi}_3\phi_4|$ is close in energy. These two determinants can be used as a basis for multireference variational AFMC of Section 2.2. In addition, one can use the UHF $S_z = 1$ open-shell determinant. Here, there is no contamination from the singlet state and higher spin states are better separated from the triplet ground state. Using this determinant allows an independent way to estimate the STED. The results of these two computations are shown in Fig. 2. It is seen that both computations lead to a similar STED. In order to determine the $\beta \to \infty$ limit, we use the fact that the asymptotic behavior is exponential:

$$J(\beta) = \Delta J \mathrm{e}^{-A\beta} + J_\infty. \qquad (20)$$

In order to estimate the statistical error, we calculated the transient $J(\beta)$ five statistically independent times. Each run employed 600 iterations. Following each run, a fit is made to the computed transient $J(\beta)$ to determine the parameters J_∞ ΔJ and A of Eq. (20). The statistics is then made on the parameters, and the result for the STED is $\boldsymbol{J}_\infty = -14.3 \pm 0.1$ kcal/mol for the UHF calculation. It is worthwhile to comment that the correlation energy contribution to J is very small (order of 1 kcal/mol) when the 2-state UHF computation is used. This is very different from the situation in the next application, where the correlation energy is a huge contribution to J.

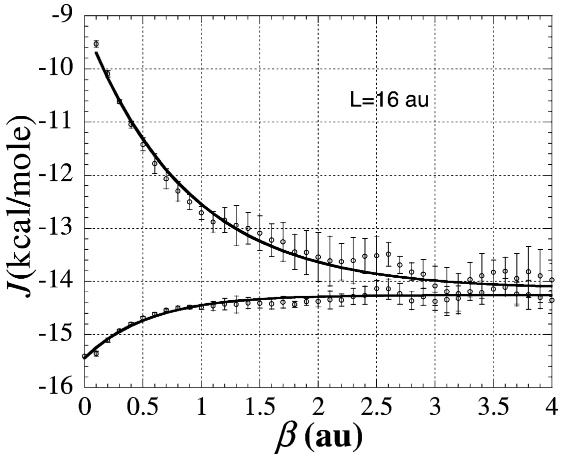

Fig. 2. Two independent ways to compute the STED J for the H–He–H benchmark system (see text for details). Solid lines are exponentials obtained by best fit. Total of 3000 iterations.

3.2. Singlet–triplet energy differences in methylene

The methylene radical (CH_2) is a classical benchmark system of quantum chemistry, where theoretical predictions, initially contradicting with experimental results, were later shown to be correct [24]. The STED was also an issue of great debate between theory and experiment.

We approached the CH_2 system, using the experimentally known C_{2v} geometries [25]: for the triplet state we take $R_{\mathrm{CH}} = 1.075$ Å and $\theta_{\mathrm{HCH}} = 133.9°$ and for the singlet, $R_{\mathrm{CH}} = 1.107$ Å and $\theta_{\mathrm{HCH}} = 102.4°$. We first performed Hartree–Fock computations to obtain, for each spin state, the determinantal wavefunction to be used as references for the QMC process. The references for the singlet and triplet states were the closed-shell $(S = 0)$ restricted Hartree–Fock (RHF) and the $S_z = 1$ unrestricted Hartree–Fock (UHF) determinants, respectively. There is no need to form a pure triplet state here because the Monte Carlo procedure will automatically distil it from other mixed $S > 0$ states. It is important to refrain from using the $S_z = 0$ UHF determinantal wavefunction as a reference for the singlet computation. This is because the triplet ground state is mixed into it, and the QMC process will only enhance the triplet contribution.

How sensitive is the computational result to cell size and grid spacing? A qualitative answer can be obtained by considering the issue at the Hartree–Fock level, as shown in Fig. 3. Both cell-size and grid spacing convergence is fast and the $\Delta x = 0.33$ Bohr and $L = 16$ Bohr combination is accurate for practical chemical purposes. Yet, this basis is much too demanding and we chose $\Delta x = 0.4$ Bohr and $L = 12$ Bohr ($L^{-1} = 0.083$ Bohr^{-1}). On the Hartree–Fock level, choosing this basis leads to an S–T energy difference which is about 0.6 kcal/mol too large.

The SC-AFMC computation proceeds as follows. First, reference states for the triplet and singlet states are produced using Hartree–Fock

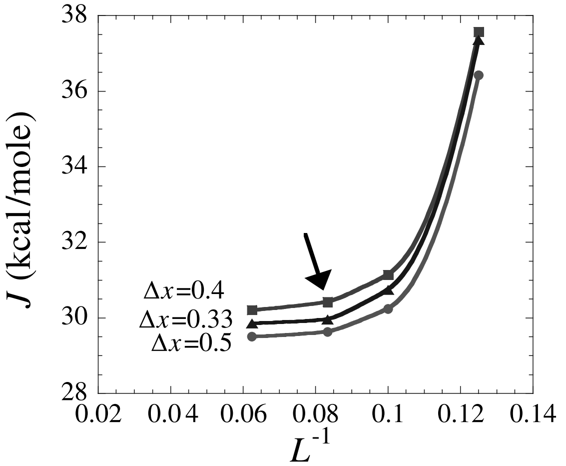

Fig. 3. Hartree–Fock triplet–singlet energy difference of methylene at the experimental geometries as a function of cubic cell length L and grid spacing Δx (both in Bohr). The arrow points to the configuration chosen for the Monte Carlo computation, $L = 12$ Bohr and $\Delta x = 0.4$ Bohr.

theory. For the triplet, an unrestricted Hartree–Fock (UHF) determinant is obtained, containing the orbitals

$$\Psi_{^3\mathrm{B}_1} = \left|(1\mathrm{a}_1)^2(1\mathrm{b}_2)^2(2\mathrm{a}_1)(1\mathrm{b}_1)\right|. \tag{21}$$

As for the singlet reference, the lowest energy RHF determinant (at the singlet geometry) is

$$\Psi_{^1\mathrm{A}_1} = \left|(1\mathrm{a}_1)^2(1\mathrm{b}_2)^2(2\mathrm{a}_1)^2\right|. \tag{22}$$

These two determinants, respectively, possess the same symmetry as the triplet and singlet ground state wavefunctions [26]. With each of them as references, we ran SC-AFMC to compute the corresponding energies. For reducing the statistical noise in the STED, the two computations are correlated by using the same auxiliary fields. Here we explicitly exploit the fact that the auxiliary fields are sampled in a spin independent way and implicitly rely on the resemblance of the corresponding shapes of the molecular orbitals. However, this is not a perfect resemblance especially due to the different nuclear configurations and spin arrangements. Thus, the correlated sampling is less effective than, say, for a force computation [5]. The result of this computation is shown in Fig. 4 where the STED is plotted as a function of β.

Following reference [Sherrill, 1998 #163] we tried to include a low-lying singlet state with the reference wavefunction. Within the variational SCAFMC, this meant to run a two-dimensional variational SCAFMC, with the second $^1\mathrm{A}_1$ wavefunction being [Sherrill, 1998 #163]:

$$\tilde{\Psi}_{^1\mathrm{A}_1} = \left|(1\mathrm{a}_1)^2(1\mathrm{b}_2)^2(2\mathrm{b}_1)^2\right|. \tag{23}$$

The results of the ensuing computation are also shown in Fig. 4. Comparing the two computations, the addition of the second $^1\mathrm{A}_1$ state has considerably accelerated the convergence of the computation. A propagation time of $\beta_{\mathrm{fin}} = 3$ a.u. is sufficient. Once again, treating the non-dynamical correlation in a variational-algebraic way is essential for obtaining an accurate result.

We estimate the statistical error in a similar way to that done for the previous system, using five statistically independent runs, each employing a certain number of iterations (in this case, 6500 for

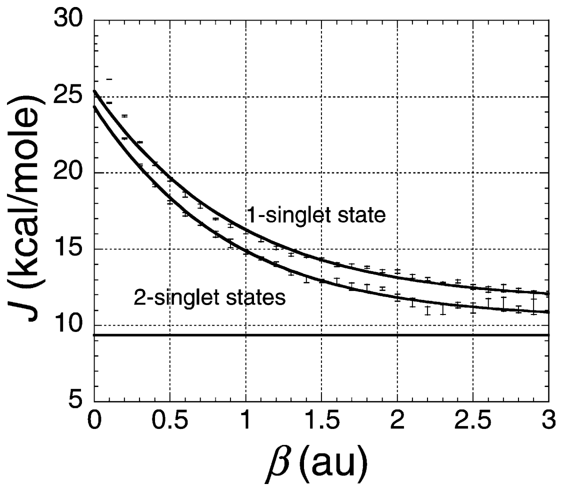

Fig. 4. Correlated sampling SC-AFMC computations of the STED for the methylene molecule. The full lines are best-fit exponentials to the Monte Carlo results for $\beta > 0.3$ a.u. Two computations are shown, with just one singlet reference and two singlet references. The horizontal line is the relevant experimental result. The extrapolated $\beta \to \infty$ value is $J = 10.4 \pm 0.3$ kcal/mol. Cell length is $L = 12$ Bohr; grid spacing $\Delta x = 0.4$ Bohr and time step is $\Delta\beta = 0.1$ a.u. Total of 20 000 Monte Carlo iterations.

the single reference and 3500 for the double reference). For each run, a fit is made to determine the parameters J_∞ ΔJ and A of Eq. (20). Statistics is again made on the parameters, and the result for the STED is $\boldsymbol{J}_\infty = -10.4 \pm 0.3$ kcal/mol. Our final estimate for J_∞ takes into account the representation error, which we estimate from the Hartree–Fock computation to be −0.6 kcal/mol (Fig. 3). Thus our final estimate for the STED is $\boldsymbol{J} = -9.8 \pm 0.3$ kcal/mol, which should be compared to the relevant experimental value of $J = 9.4$ kcal/mol [27,28].

The only uncontrolled approximation in our method is that of using the pseudopotential. We have tested, at the Hartree–Fock level, six different density functional – based pseudopotentials. Three of them use the local density approximation (LDA) and the other three – various versions of the generalized gradients approximation (GGA). It was found that results derived from various LDA-based pseudopotentials are similar (to within 0.5 kcal/mol) and the same is seen for the GGA-based pseudopotentials. However, the results derived from LDA-based pseudopotentials were consistently higher by 2 kcal/mol than those derived from the GGA-based ones. We compared two AFMC computations: one using the LDA-based pseudopotential and the other – that based on GGA. It was seen that the energetic difference observed at the Hartree–Fock level is closely preserved also in the correlated computation. Thus, within a given model for the nucleus, there is little difference as to what exact form of a functional was taken, but between the two models, the difference is larger. Thus, the pseudopotential uncertainty dominates the accuracy in our calculation. Furthermore, the results derived from the GGA-based pseudopotentials were in close agreement with the experimental results (to within statistical uncertainty), while those derived from LDA-based pseudopotentials give a poor fit to experiment.

4. Summary

The shifted contour auxiliary field Monte Carlo method is shown to be able to accurately compute electronic excited state energy differences, namely the singlet–triplet differences of small benchmark molecules. The methods for achieving this feat include a variational multireference version of AFMC for dealing with non-dynamical correlation and the concept of correlated sampling for different spin states.

In this work, the unrestricted Hartree–Fock was used for constructing the optimized determinants reference states of the AFMC process. An alternative, more standard approach, consists of constructing triplet references from a linear combination of two triplet-paired determinants. In a future study, we intend to compare these two approaches to the computation of triplet state energies.

Finally, we have found that the uncontrolled source of error in our computation – the pseudopotential – can dominate the accuracy. Specifically, we find that results derived from GGA based pseudopotentials agree closely with experiment while those derived from LDA-based pseudopotentials yield a discrepancy of 10–20%.

Acknowledgements

This work was supported by Israel Science Foundation founded by the Israel Academy of Sciences and Humanities. I gratefully thank J.M.L. Martin and S. Shaik for their help and encouragement.

References

[1] W. Heisenberg, Z. Phys. 49 (1928) 619.

[2] J.R. Hart, A.K. Rappe, S.M. Gorun, T.H. Upton, J. Phys. Chem. 96 (1992) 6255.

[3] N. Rom, D.M. Charutz, D. Neuhauser, Chem. Phys. Lett. 270 (1997) 382.

[4] R. Baer, M. Head-Gordon, D. Neuhauser, J. Chem. Phys. 109 (1998) 6219.

[5] R. Baer, J. Chem. Phys. 113 (2000) 473.

[6] R. Baer, Chem. Phys. Lett. 324 (2000) 101.

[7] L. Noodleman, J. Chem. Phys. 74 (1981) 5737.

[8] E. Ruiz, J. Cano, S. Alvarez, P. Alemany, J. Comput. Chem. 20 (1999) 1391.

[9] B. Bernu, D.M. Ceperley, W.A. Lester, J. Chem. Phys. 93 (1990) 552.

[10] N. Rom, E. Fattal, A.K. Gupta, E.A. Carter, D. Neuhauser, J. Chem. Phys. 109 (1998) 8241.

[11] R. Baer, D. Neuhauser, J. Chem. Phys. 112 (2000) 1679.

[12] P.L. Silvestrelli, S. Baroni, R. Car, Phys. Rev. Lett. 71 (1993) 1148.

[13] D.M. Charutz, D. Neuhauser, J. Chem. Phys. 102 (1995) 4495.

[14] G.J. Martyna, M.E. Tuckerman, J. Chem. Phys. 110 (1999) 2810.

[15] A.D. Becke, Phys. Rev. A 38 (1988) 3098.

[16] C.T. Lee, W.T. Yang, R.G. Parr, Phys. Rev. B 37 (1988) 785.

[17] N. Troullier, J.L. Martins, Phys. Rev. B 43 (1991) 1993.

[18] M. Fuchs, M. Scheffler, Comput. Phys. Commun. 119 (1999) 67.

[19] L. Kleinman, D.M. Bylander, Phys. Rev. Lett. 48 (1982) 1425.

[20] R. Caballol, O. Castell, F. Illas, P.R. Moreira, J.P. Malrieu, J. Phys. Chem. A 101 (1997) 7860.

[21] J.R. Hart, A.K. Rappe, S.M. Gorun, T.H. Upton, J. Phys. Chem. 96 (1992) 6264.

[22] A. Bencini, F. Totti, C.A. Daul, K. Doclo, P. Fantucci, V. Barone, Inorg. Chem. 36 (1997) 5022.

[23] J.M. Martin, Private Communication, 2000.

[24] H.F. Schaefer, Science 231 (1986) 1100.

[25] H. Petek, D.J. Nesbitt, D.C. Darwin, P.R. Ogilby, C.B. Moore, D.A. Ramsay, J. Chem. Phys. 91 (1989) 6566.

[26] M.E. Jacox, J. Phys. Chem. Ref. Data (1994) 1.

[27] C.D. Sherrill, M.L. Leininger, T.J. Van Huis, H.F. Schaefer, J. Chem. Phys. 108 (1998) 1040.

[28] P. Jensen, P.R. Bunker, J. Chem. Phys. 89 (1988) 1327.